Focusing inversion of marine full-tensor gradiometry data in offshore geophysical exploration

Le Wan and Michael S. Zhdanov, Consortium for Electromagnetic Modeling and Inversion, University of Utah*

Summary

In this paper we demonstrate that marine gravity gradiometry data can be effectively used for offshore hydrocarbon exploration. We apply a three-dimensional (3D) focusing inversion method to interpretation of the marine full-tensor gradient (FTG) data collected in the Barents Sea. We conduct inversion of the different individual components and a joint inversion of several FTG components. The numerical results demonstrate that the joint inversion helps to produce a consistent 3D model of the anomalous density distribution in the area of the FTG survey. The results of 3D inversion of FTG data show a possibility for resolving the complex geological structures of salt diapir formations using gravity gradiometry data.

Introduction

Recent technological developments make it possible to accurately measure all the independent tensor components of the gravity gradient field from a moving platform. In this paper we consider a method of interpretation of marine full-tensor gradiometry (FTG) data.

Inversion of tensor gravity gradient data is complicated by the fact that the gravity data are invariably contaminated by noise and are acquired at a limited number of observation points. Therefore, inversion of these data represents a typical ill-posed problem. The solution of an ill-posed problem requires the application of corresponding regularization methods (Tikhonov and Arsenin, 1977). The traditional way to implement regularization in the solution of an inverse problem is based on a consideration of the class of inverse models having a smooth distribution of the model parameters. Within the framework of classical Tikhonov regularization, one can select a smooth solution by introducing the corresponding minimum-norm, or "smoothing," stabilizing functionals. This approach is widely used in geophysics and has proven to be a powerful tool for stable inversion of geophysical data.

The traditional inversion algorithms providing smooth solutions for geological structures have difficulties, however, in describing the sharp boundaries between different geological formations. In these situations, it is useful to search for a stable solution within the class of inverse models with sharp petrophysical boundaries.

The mathematical technique for solving this problem is described in detail in the monograph by Zhdanov (2002). It is based on introducing a special type of stabilizing functionals, the so-called minimum-support or minimum-gradient support functionals (Portniaguine and Zhdanov, 1999, 2002). This technique is called a focusing regularized inversion to distinguish it from the traditional smooth regularized inversion.

In this paper we consider an application of the focusing inversion to the interpretation of the marine full-tensor gradient (FTG) data collected in the Barents Sea.

Tensor gravity gradiometer data

Here we provide a brief mathematical description of the gravity tensor components (after Zhdanov et al., 2004), which are measured by marine gravity gradiometers.

The second spatial derivatives of the gravity potential $U(\mathbf{r})$ form a symmetric *gravity tensor*:

$$\hat{\mathbf{g}} = \begin{bmatrix} g_{xx} & g_{xy} & g_{xz} \\ g_{yx} & g_{yy} & g_{yz} \\ g_{zx} & g_{zy} & g_{zz} \end{bmatrix},$$

where

$$g_{\alpha\beta}(\mathbf{r}) = \frac{\partial^2}{\partial\alpha\partial\beta}U(\mathbf{r}), \quad \alpha,\beta = x,y,z, \tag{1}$$

and

$$U(\mathbf{r}) = \gamma \iiint_D \frac{\rho(\mathbf{r}')}{|\mathbf{r}'-\mathbf{r}|}\,\mathbf{dv}'. \tag{2}$$

The expressions for the gravity tensor components can be calculated based on formulae (1) and (2):

$$g_{\alpha\beta}(\mathbf{r}) = \gamma \iiint_D \frac{\rho(\mathbf{r}')}{|\mathbf{r}'-\mathbf{r}|^3} K_{\alpha\beta}(\mathbf{r}'-\mathbf{r})\,dv', \tag{3}$$

where kernels $K_{\alpha\beta}$ are equal to:

$$K_{\alpha\beta}(\mathbf{r}'-\mathbf{r}) = \begin{cases} 3\frac{(\alpha-\alpha')(\beta-\beta')}{|\mathbf{r}'-\mathbf{r}|^2}, \alpha \neq \beta \\ 3\frac{(\alpha-\alpha')^2}{|\mathbf{r}'-\mathbf{r}|^2} - 1, \ \alpha = \beta \end{cases}, \quad \alpha,\beta = x,y,z. \tag{4}$$

Using formulae (3) and (4), derived above, we can present the gravity tensor components in discretized form, convenient for numerical modeling and inversion.

Focusing inversion of full-tensor gradiometry data

In a general case, the gravity inverse problem can be expressed by an operator equation:

$$d = A\,(m)\,, \tag{5}$$

where A is a forward modeling operator, $m = m(\mathbf{r})$ is a scalar function describing the distribution of the density in some volume V in the earth, and $d = d(\mathbf{r})$ is a gravity gradiometer data set formed by observed values of the corresponding components of the gravity gradiometry tensor.

Inversion aims at determining the model parameters m based on A and some known (observed) data d. This problem is usually ill posed, i.e., the solution can be nonunique and unstable. The conventional way of solving ill-posed inverse problems, according to regularization theory, is based on minimization of the Tikhonov parametric functional:

$$P^{\alpha}(m) = \phi(m) + \alpha s(m) = \min, \tag{6}$$

where $\phi(m)$ is a misfit functional determined as a norm of the difference between observed and predicted data, functional $s(m)$ is a stabilizing functional (a stabilizer), and α is a regularization parameter.

The stabilizing functional incorporates information about the basic properties of the types of models used in the inversion. The traditional smooth inversion algorithms are based on the minimum-norm or maximum-smoothness stabilizing functionals (e.g., Occam's inversion). These stabilizers produce smooth geological models, which in many practical situations do not describe properly the blocky geological structures.

In order to produce focused images of a target with sharp boundaries, we use a new type of stabilizing functional, the so-called minimum-support or minimum-gradient support functional (Zhdanov, 2002):

$$s_{MS}(m) = \iiint_V \frac{(m - m_{apr})^2}{(m - m_{apr})^2 + e^2} dv. \tag{7}$$

The minimization problem (6) is solved using the re-weighted regularized conjugate-gradient (RRCG) method, which was outlined in Zhdanov (2002, pp. 155-165).

Geological characteristic of the area of a 3D marine FTG survey

The FTG survey was conducted with-in the Nordkapp Basin in the Barents Sea, offshore Norway. Hydrocarbon (HC) exploration in the Nordkapp Basin started in the 1980s. The recent results of geological and geophysical exploration and the discovery of hydrocarbons in wells outside the basin indicate that there is a potential for HC reservoir discovery within the Nordkapp Basin.

The complex salt diapirs represent the major geological structures known in this area (see Figure 1). Much of the present uncertainty and exploration risk associated with these salt features result from severe seismic imaging distortion problems and subsequent interpretation ambiguity of the salt isopach (specifically the ability to seismically define/map the salt base). The goal of the FTG survey was to provide additional information for evaluation of these complex salt overhang geometries. FTG, by its very nature, is very well suited to solve this problem. It can be used to define geological boundaries with strong density contrasts, typical for salt-diapir structures.

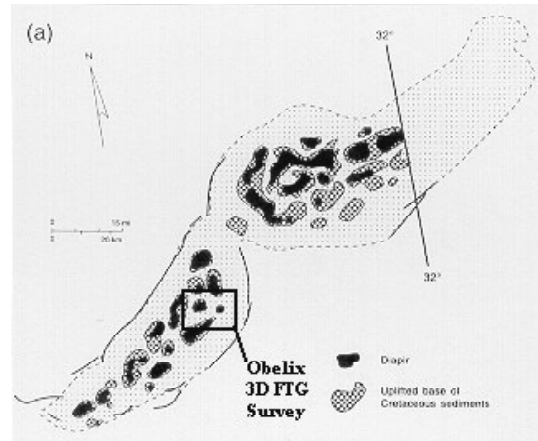

Fig. 1: Simplified structural map of the Nordkapp Basin showing salt diapirs and main fault zones. The black zones show subcrops of diapirs at or near the Pliocene-Pleistocene unconformity.

However, in order to adequately solve this problem, a rigorous 3D inversion should be applied to the FTG data. In order to find the sharp boundaries of the salt domes, it is necessary to use the method of focusing inversion. In this paper we present the preliminary results of this inversion using the focusing regularization, which is capable of resolving the sharp density contrast between the salt structures and the surrounding host rocks.

Inversion results for single components of the gravity tensor

We have applied the focusing inversion first to different single components of the gravity tensor. The main geological targets are the salt diapirs G2 and F2 (see Figure 2). We have selected from the original data set a subset of the FTG data to focus on these two salt diapir areas. We present the inversion results in the form of the vertical sections along profile B-B' shown in Figure 3.

We run the inversion for the following single components of the gravity tensor: g_{xz}, g_{yz}, and g_{zz}. We have selected a modeling domain 28 km (east-west) $\times$17 km (north-south) and extended at a depth of 6 km. This volume of inversion was discretized in $281 \times 171 \times 60 = 2,883,060$ cells; the cell size is 100 m $\times$100 m $\times$100 m. Thus, the selected modeling domain may represent a salt base or a deeper source down to approximately 6 km for salt structures F1 and G2.

A typical density of the base tertiary rocks in the area of investigation is within 2.30-2.38 g/cm^3. The salt diapirs are characterized usually by negative density anomalies. The following Figures 4-6 show the vertical slices of the inversion results along the profile B-B'. One can clearly see the salt diapir G2 in these single component inversion

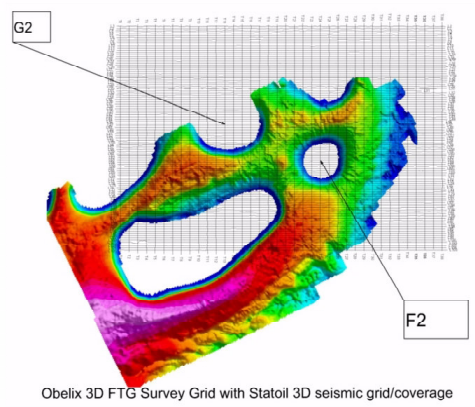

Fig. 2: 3D FTG survey grid with 3D seismic grid coverage.

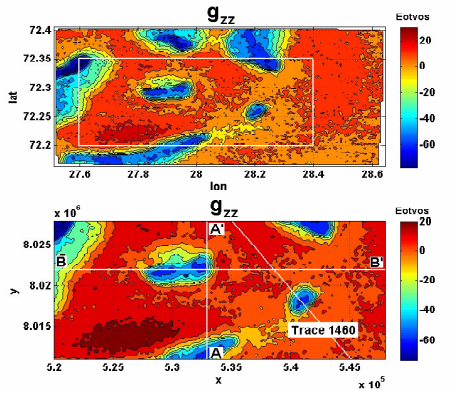

Fig. 3: Maps of the g_{zz} component of the full-tensor gradiometry (FGT). The white line in the top panel outlines the rectangular area selected for the focusing inversion. The bottom panel shows the location of the A-A' and B-B' profiles.

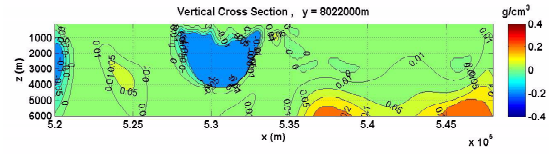

Fig. 4: A vertical section of the inversion result for the g_{zz} component along the B-B' profile.

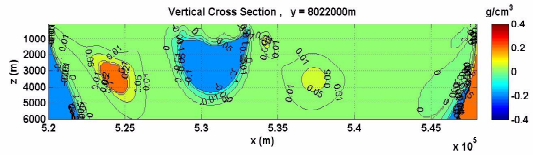

Fig. 5: A vertical section of the inversion result for the g_{xz} component along the B-B' profile.

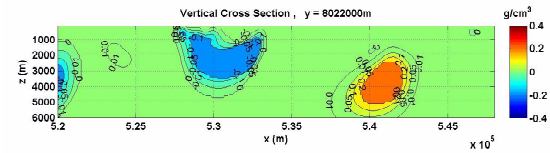

Fig. 6: A vertical section of the inversion result for the g_{yz} component along the B-B' profile.

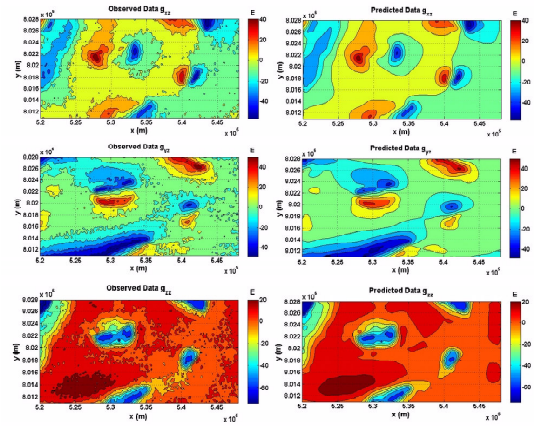

Fig. 7: Maps of the observed and predicted FTG data for the different components (g_{zz}, g_{xz}, and g_{yz}) of the full tensor.

results. However, the results obtained for different components are slightly different. Figure 7 shows the maps of the observed and predicted FTG data for the different components g_{zz}, g_{xz}, and g_{yz} of the full tensor. We can see in these maps that the predicted data fit the observed data very well. An average misfit between the observed and predicted data is within 1%.

Joint inversion results

We have inverted jointly two components and three components of the TGF tensor. We use the same discretization in the joint inversion as was used in the single component inversion. Figure 8 shows the joint inversion results for the g_{zz} and g_{xz} components in the form of vertical sections along the profile B-B'. One can clearly see the location of the salt diapir G2 in these figures.

Finally, we present the results of the joint inversion of three components of the gravity tensor: g_{zz}, g_{xz}, and g_{yz}.

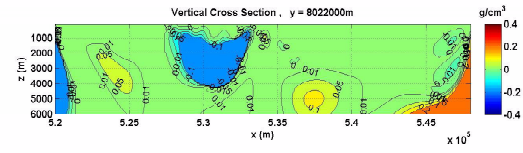

Fig. 8: A vertical section of the joint inversion result for the g_{zz} and g_{xz} components along the B-B' profile.

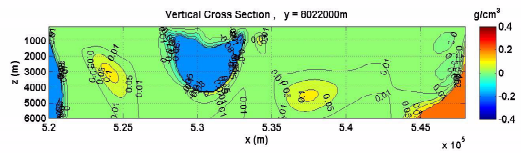

Fig. 9: A vertical section of the joint inversion results for the g_{zz}, g_{xz}, and g_{yz} components along the B-B' profile.

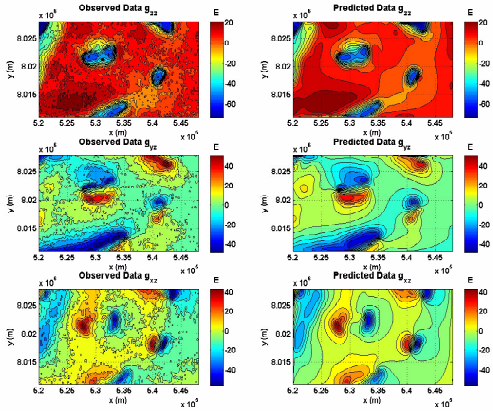

Fig. 10: Maps of the observed and predicted data for the results of the joint inversion of the g_{zz}, g_{xz}, and g_{yz} components of the FTG survey.

The plot in Figure 9 shows the inverted density distribution along the profile B-B'.

Figure 10 presents a comparison between the observed and predicted data for the case of joint g_{zz}, g_{xz}, and g_{yz} inversion. The predicted data agree very well with the observed data.

For comparison, we present in Figure 11 the joint inversion result for three FTG components along the Trace 1460 profile.

Figure 12 shows the same result overlapped with the seismic depth migration section. We can clearly see the salt diapir F2 both in the density section and in the seismic section along this profile.

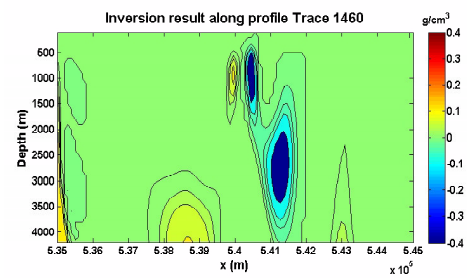

Fig. 11: The joint inversion results for the three FTG components along Trace 1460.

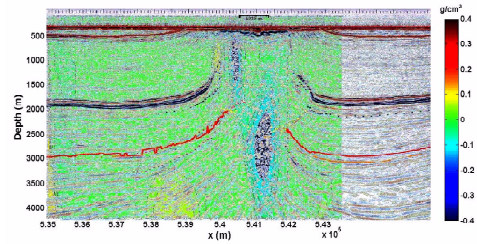

Fig. 12: The joint inversion results for the three FTG components overlapped with the seismic depth migration section.

Conclusions

We have demonstrated in this paper that the marine full-tensor gradiometry (FTG) survey is very sensitive to the density distribution in geological formations. The gravity tensor components represent well the density anomalies associated with complex salt diapirs and their related structural traps. The 3D inversion of FTG data makes it possible to resolve the complex geological structures of salt formations. We have run inversion of the individual components of the full gravity gradient tensors, and we have also applied a joint inversion. The numerical results demonstrate that the joint inversion helps to "clean up" the inverse image and to produce a consistent 3D model of the density distribution in the area of the FTG survey.

The focusing inversion also helps to determine the fine details of the salt diapirs, from wide salt stocks with vertical flanks to more complex geometries with broad diapir overhangs above narrow stems. This practical example of marine FTG data interpretation clearly illustrates the importance of the 3D focusing inversion in the effective interpretation of gravity gradiometry data.

Acknowledgments

The authors acknowledge the support of the University of Utah Consortium for Electromagnetic Modeling and Inversion (CEMI).

We are thankful to Dr. Brian Farrelly and StatoilHydro for providing the gravity gradiometer data and for permission to publish the results.

EDITED REFERENCES

Note: This reference list is a copy-edited version of the reference list submitted by the author. Reference lists for the 2008 SEG Technical Program Expanded Abstracts have been copy edited so that references provided with the online metadata for each paper will achieve a high degree of linking to cited sources that appear on the Web.

REFERENCES

Portniaguine, O., and M. S. Zhdanov, 1999, Focusing geophysical inversion images: Geophysics, **64**, 874–887.

———2002, 3D magnetic inversion with data compression and image focusing: Geophysics, **67**, 1532–1541.

Tikhonov, A. N., and V. Y. Arsenin, 1977, Solution of ill-posed problems: Winston and Sons.

Zhdanov, M. S., 2002, Geophysical inverse theory and regularization problems: Elsevier.

Zhdanov, M. S., R. G. Ellis, and S. Mukherjee, 2004, Regularized focusing inversion of 3D gravity tensor data: Geophysics, **69**, 925–937.